# Retrieving the Vertical Profile of Cloud Droplet Effective Radius from Multiple Spectral Channels

*F.-L. Chang and Z. Li*
*Canada Centre for Remote Sensing*
*Ottawa, Ontario, Canada*

*H. W. Barker*
*Atmospheric Environment Service*
*Dowsview, Ontario, Canada*

## Introduction

Cloud optical depth and droplet size are two important parameters required for understanding the radiative effects of clouds and their impact on climate (e.g., Fouquart et al. 1990). Numerous efforts have been made to retrieve the two parameters from remote sensing and compare them with in situ measurements (e.g., Stephens and Tsay 1990). Usually, the visible channel measurement is used to retrieve cloud optical depth ($\tau$) and a near-infrared (NIR) channel to retrieve cloud effective droplet radius ($r_e$) (Hansen and Travis 1974). While aircraft (e.g., Nakajima and King 1990) and surface-based (e.g., Twomey and Cocks 1982) studies used 1.6 μm and 2.2 μm radiance measurements to retrieve $r_e$, much attention has also been focused on the use of National Oceanic and Atmospheric Administration (NOAA) Advanced Very High Resolution Radiometer (AVHRR) satellite measurements at 3.7 μm for retrieving $r_e$ (e.g., Han et al. 1994). Note that these retrievals of $r_e$ only represent a very thin layer near cloud top.

In this paper, we propose a scheme for inferring the vertical distribution of $r_e$ in an optically thick cloud layer. The current scheme explores the use of reflected solar radiances from four NIR spectral channels and one visible channel to retrieve $r_e$ at various optical depth levels. The $r_e$ at different optical depth levels can be linked to actual vertical elevations from cloud profiling radar (CPR) such as those deployed in the Atmospheric Radiation Measurement (ARM) Program or from a space-borne CPR mission such as CloudSat (Stephens 1998).

Using model simulations of solar reflectances for cloud layers composed of various optical depths and droplet effective radii, the retrievals of $\tau$ and $r_e$ with the current and conventional schemes are compared with input true values. The applicability of the current scheme and improvement over the conventional ones are also discussed.

## Theory and Radiation Model

An adding-doubling plane-parallel radiative transfer model was used to simulate the solar reflectances that would be observed by a satellite sensor at one visible 0.63-μm channel and four NIR channels: 1.25 μm, 1.65 μm, 2.15 μm, and 3.75 μm. Satellite measurements at the above atmospheric window channels will become available soon from the Moderate Resolution Imaging Spectrometer (MODIS, Salomonson et al. 1989) of the Earth Observing System (EOS). A standard midlatitude summer atmosphere from McClatchey et al. (1972) was used in the radiation model. The atmosphere was divided into eight vertical layers with the cloud layer placed between 1 km and 2 km. Mie theory was used to account for the absorption and scattering of cloud droplets with a gamma size distribution. LOWTRAN7 model was used to correct for the atmospheric absorption and scattering. Lambertian surface reflectance of 0.06 was used for all spectral wavelengths. The bi-directional reflectances were calculated at discrete cloud visible optical depths and droplet effective radii.

Figure 1 shows the bi-directional reflectances at the top of the atmosphere calculated for various cloud properties at the five channels. At 0.63-μm visible wavelength (bottom figure), cloud droplets are non-absorbing. Sunlight penetrates deeply into the cloud and photons undergo many scattering events before exiting the cloud. Visible radiances reflected by cloud depend primarily on cloud optical depth. The retrievals of cloud optical depths from visible reflectances are fairly reliable with an uncertainty of 15% to 25% for water clouds, even in the absence of cloud microphysical information (Rossow et al. 1989). At 1.25 μm to 3.75 μm NIR wavelengths, however, the reflectances become very sensitive to the droplet size. The reflectance may saturate as $\tau$ increases. This is because cloud droplets are absorbing at these wavelengths. The single-scattering albedo ($\omega_o$) decreases with increasing droplet effective radius, so that larger droplets saturate faster than smaller droplets. Due to the strong dependence of $\omega_o$ on both the wavelength and droplet size, cloud reflectance at NIR wavelengths can, therefore, be used to infer the droplet size.

If $r_e$ is non-uniform vertically, the retrieval of $r_e$ is spectral sensitive. For instance, at 3.75-μm wavelength, co-single-scattering albedo ($1-\omega_o$) is relatively large (~0.045 for $r_e$ = 5 μm; ~0.186 for $r_e$ = 24 μm). Photons get absorbed quickly by cloud droplets after few times of scattering. The photon trajectories are short and so the retrieved droplet effective radius represents the value from the top portion of a cloud. At shorter wavelengths, $1-\omega_o$ is relatively small (e.g., at 1.25-μm, ~0.0008 for $r_e$ = 5 μm and ~0.0035 for $r_e$ = 24 μm). Thus, photons can penetrate deep inside the cloud. The retrieved $r_e$ thus represents the value for a deeper cloud column. Thus, the reflectance variation among NIR wavelengths can be used to infer the vertical profile of the droplet effective radius.

## Retrieval Scheme

The scheme adopts the look-up table computed for the channels selected. The idea is to take advantage of the varying absorption properties of cloud droplet at NIR channels to vertically slice the cloud layer. Cloud is assumed to be a vertical stack of several plane-parallel layers with different cloud optical properties. The measurement at the longest wavelength (3.75 μm here) is first used to retrieve $r_e$ for the cloud top layer. With the retrieved cloud optical properties in the top layer, the retrieving process

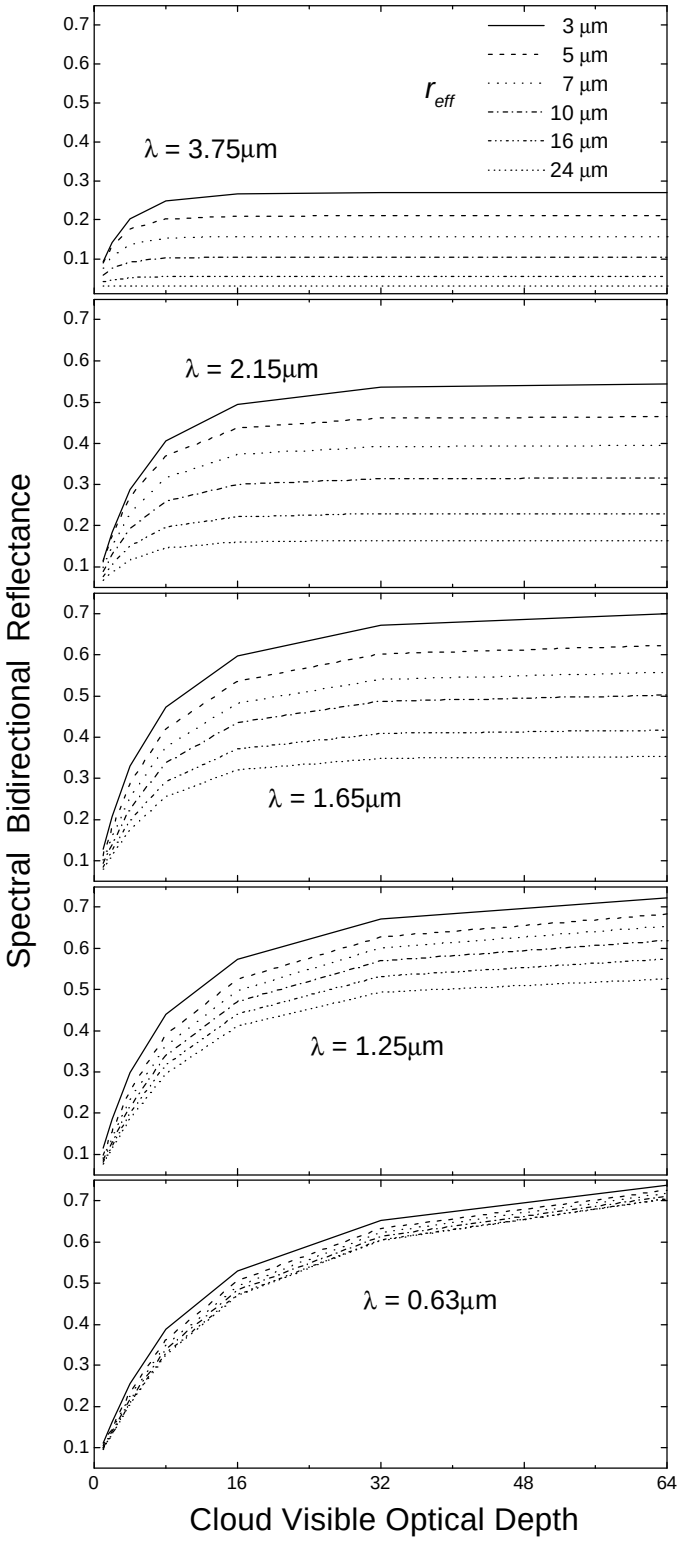


**Figure 1**. Model simulations of satellite observed bi-directional reflectances for $(\theta_0,\theta,\phi-\phi_0) = (63.1°,5.9°,0.0°)$.

proceeds to the second layer using a channel of shorter wavelength. Note that a different look-up table is employed for a two-layer cloud. A similar procedure is followed for the remaining channels.

During the retrievals, the optical depths of each layer, except the last (bottom) layer, are input variables used to determine the optical depth levels for the output of $r_e$. The optical depth and $r_e$ of the last layer is then retrieved using the visible and the shortest NIR channels, as done in conventional scheme. The total optical depth is thus the sum of all layers. Note that if the optical depth of a layer is determined thin, the look-up table needs to account for the reflectance changes due to the droplet size variation at lower layer(s). Such an adjustment can be completed by iteration using the $r_e$ inferred from shorter wavelength(s).

Figure 2 shows model simulations of observed spectral reflectance for a two-layer cloud for solar zenith angle ($\theta_o$) 63.1°, viewing zenith ($\theta$) 5.9°, and relative azimuth ($\phi$-$\phi_o$) 0°. By varying the top-layer cloud optical depth (X-axis) and the bottom-layer droplet effective radii (different line types), variations in reflectance for the four NIR channels are shown. Cloud optical depth at the bottom layer is set to be 40. Panels 2a and 2b are respectively for fixed droplet effective radii 24 μm and 5 μm for the top layer. Clearly, the 3.75-μm reflectance can only be used to retrieve the cloud-top droplet effective radius, whereas the 1.25-μm reflectance can be used to infer the droplet size below $\tau_{0.63} \sim 40$.

## Results and Discussion

To illustrate the feasibility of the retrieval scheme, reflectances at 0.63 μm, 1.25 μm, 1.65 μm, 2.15 μm, and 3.75 μm were simulated for a cloud layer composed of a vertical stack of eleven plane-parallel layers. These layers have the same $\tau_{0.63} = 4$ (total 44), but different $r_e$. Table 1 shows two profiles of $r_e$, decreasing and increasing from top to bottom layers. Both the current scheme and conventional one were applied to the simulated data. For the current retrieval scheme, the reflectance look-up tables were calculated using a cloud layer composed of four plane-parallel layers. An optical depth of 8 was used for each of the top three layers in the slicing process. The 3.75-μm, 2.15-μm, and 1.65-μm channels, therefore, were used to retrieve $r_e$, which represent the top, second, and third layers, respectively. The last, channel (1.25 μm) was used to retrieve an $r_e$ that represents the column of the last (bottom) layer. The column-integrated optical depth for the whole cloud layer can then be retrieved from 0.63-μm reflectance with known optical properties of the top three layers.

**Table 1**. Cloud visible optical depths and droplet effective radii for the eleven-layered cloud model.

| | **Cloud Layers** | | | | | | | | | | |
|---|---|---|---|---|---|---|---|---|---|---|---|
| | **Top** | **2nd** | **3rd** | **4th** | **5th** | **6th** | **7th** | **8th** | **9th** | **10th** | **Bottom** |
| $\tau_{0.63}$ (44) | 4 | 4 | 4 | 4 | 4 | 4 | 4 | 4 | 4 | 4 | 4 |
| $r_{e,1}$ (μm) | 22 | 20 | 16 | 14 | 12 | 10 | 9 | 8 | 7 | 6 | 5 |
| $r_{e,2}$ (μm) | 6 | 7 | 9 | 10 | 12 | 14 | 16 | 18 | 20 | 22 | 24 |

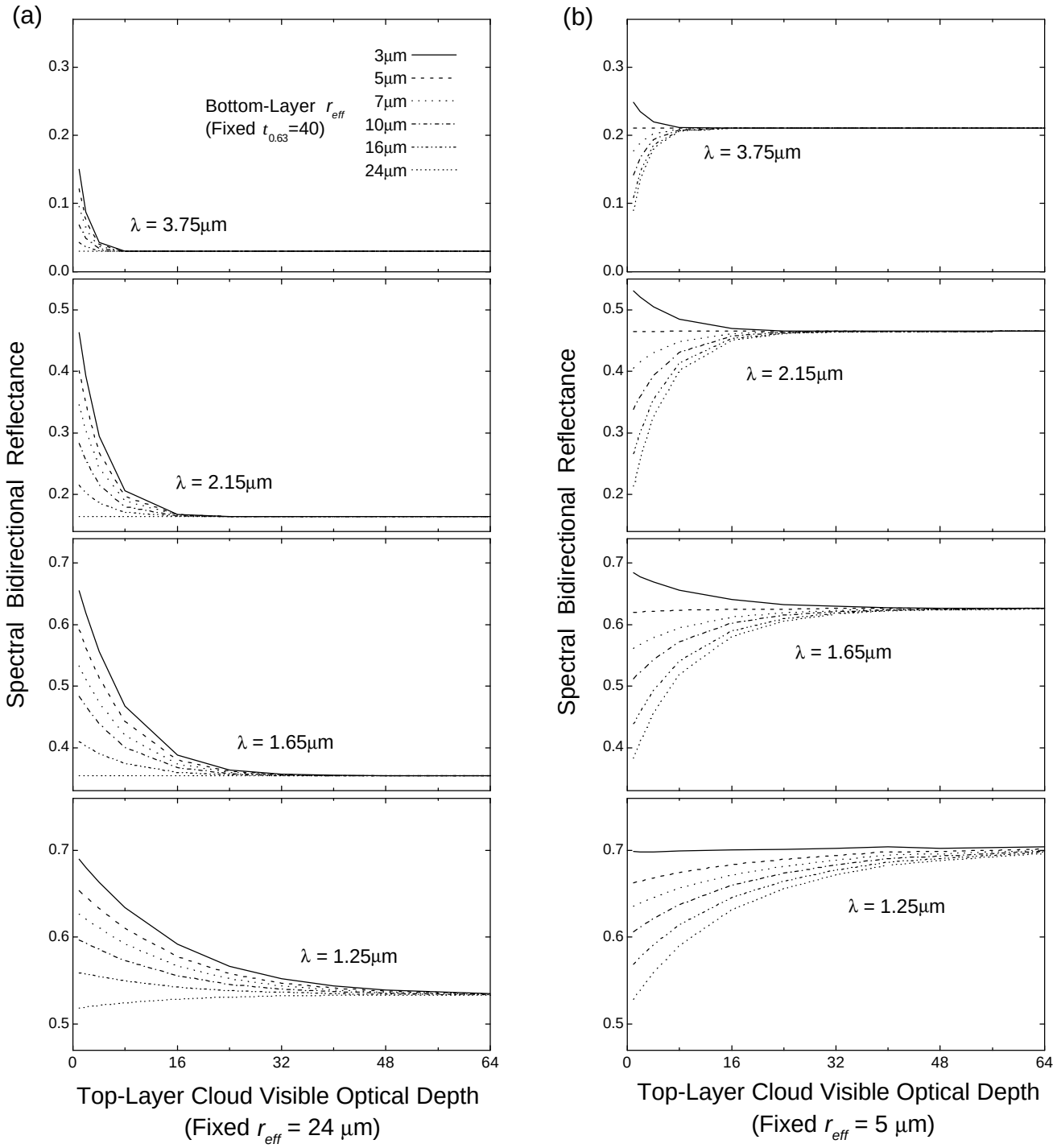


**Figure 2**. Model simulations of satellite observed bi-directional reflectances for a two-layer cloud model. Results are obtained for $(\theta_0,\theta,\phi-\phi_0) = (63.1°,5.9°,0.0°)$.

The retrievals of $\tau_{0.63}$ and layered $r_e$ for the two simulated profiles using the current scheme are shown in Table 2, in comparison with those retrieved with the conventional method. The results are given for two different solar angles near nadir. Both schemes are more effective at nadir view angles than at large view angles. The retrieved profiles of $r_e$ form the current scheme compare fairly well with the input profiles, attesting the strength of the new method. It can even infer $r_e$ at the level of $\tau_{0.63} \sim 40$ rather accurately. In contrast, the conventional method using individual NIR channel only retrieves a single "effective" $r_e$. Moreover, the column-integrated $\tau_{0.63}$ retrieved with the current method is more accurate than are those from the conventional ones. For the conventional schemes, even with the shortest 1.25-μm channel, the retrieved $r_e$ merely represents a layer of $\tau_{0.63} \sim 20$.

**Table 2**. Retrievals of cloud visible optical depths and droplet effective radii.

| | **Current Scheme** | | | | | **Conventional Scheme** | | | |
|---|---|---|---|---|---|---|---|---|---|
| Wavelength (μm) | 0.63 | 3.75 | 2.15 | 1.65 | 1.25 | 3.75/0.63 | 2.15/0.63 | 1.65/0.63 | 1.25/0.63 |
| $(\theta_o,\theta,\phi-\phi_o)$ | $\tau_{0.63}$ | $r_{eff}$ (μm) | | | | $r_{eff}$ (μm) / $\tau_{0.63}$ | | | |
| $r_{e,1}$: (5.9°,5.9°,0°) | 44.6 | 21.7 | 15.2 | 10.2 | 7.4 | 21.9 / 47.7 | 20.5 / 47.2 | 18.0 / 46.5 | 15.1 / 4.8 |
| $r_{e,1}$: (63.1°,5.9°,0°) | 43.9 | 22.0 | 15.0 | 10.4 | 7.9 | 22.2 / 47.0 | 21.3 / 46.9 | 18.8 / 46.5 | 15.8 / 45.9 |
| $r_{e,2}$: (5.9°,5.9°,0°) | 43.1 | 6.4 | 9.3 | 13.4 | 19.9 | 6.4 / 40.8 | 7.1 / 41.7 | 7.8 / 42.3 | 8.9 / 43.1 |
| $r_{e,2}$: (63.1°,5.9°,0°) | 43.7 | 6.3 | 10.4 | 13.0 | 18.7 | 6.2 / 40.7 | 6.8 / 41.4 | 7.6 / 42.1 | 9.0 / 43.1 |

While the current method infers $r_e$ at different optical depth levels, the actual elevation is unknown. The cloud top height can often be inferred from infrared channels (e.g., 11 μm), but the determination of cloud bottom and vertical extent from remote sensing is difficult. The problem can be resolved if CloudSat is launched (Stephens 1998).

## Acknowledgment

This work was supported by Research Grant No. DE-FG02-97ER62361, from U.S. Department of Energy.

## References

Fouquart, Y., J. C. Buriez, M. Herman, and R. S. Kandel, 1990: The influence of clouds on radiation: A climate-modeling perspective. *Rev. Geophys.*, **28**, 145-166.

Han, Q., W. B. Rossow, and A. A. Lacis, 1994: Near-global survey of effective droplet radii in liquid water clouds using ISCCP data. *J. Climate*, **7**, 465-497.

Hansen, J. E., and L. D. Travis, 1974: Light scattering in planetary atmospheres. *Space Sci. Rev.*, **16**, 527-610.

Nakajima, T., and M. D. King, 1990: Determination of the optical thickness and effective particle radius of clouds from reflected solar radiation measurements. Part I: Theory. *J. Atmos. Sci.*, **47**, 1878-1893.

Rossow, W. B., L. C. Garder, and A. A. Lacis, 1989: Global, seasonal cloud variations from satellite radiance measurements. Part I: Sensitivity of analysis. *J. Climate*, **2**, 419-458.

Salomonson, V. V., W. L. Barnes, P. W. Maymon, H. E. Montgomery, and H. Ostrow, 1989: MODIS: Advanced facility instrument for studies of the earth as a system. *IEEE Trans. Geosci. Remote Sens.*, **27**, 145-153.

Stephens, G., 1998: CloudSat Science Document.

Stephens, G., and S.-C. Tsay, 1990: On the cloud absorption anomaly. *Quart. J. Roy. Meteor. Soc.*, **116**, 671-704.

Twomey, S., and T. Cocks, 1982: Spectral reflectance of clouds in the near-infrared: Comparison of measurements and calculations. *J. Meteor. Soc. Japan*, **60**, 583-592.